V International Scientific and Technical Conference Actual Issues of Power Supply Systems

Ensuring the stability of the “construction-base” system under the influence of dynamic forces

AIPCP25-CF-ICAIPSS2025-00418 | Article

Ensuring the stability of the “construction-base” system under the influence of dynamic forces

Daniyar Paluanov[1,a)], Feruza Aytbaeva[2], Farid Saidov[1], Azamat Mambetov[1]

[1]*Tashkent state technical university named after Islam Karimov, Tashkent, Uzbekistan*
[2]*Scientific Research Institute of Irrigation and Water Problems, 100187 Tashkent, Uzbekistan*

[a)] *Corresponding author: doni_pol@mail.ru*

Abstract. During the many years of operation of the water discharge structure into the Birlik Canal, various deformations occurred in the body and elements of the structure. During operation, as a result of the movement of various types of heavy and light vehicles over the structure under the influence of dynamic forces, vertical settlement processes occurred in the body and foundation of the structure. Vertical subsidence was especially intense in the lower part of the structure's ridge. Dynamic forces led to the formation of cracks in the concrete, vibration of shut-off mechanisms, weakening of fasteners, and, most notably, the loss of structural stability. Therefore, it is essential to ensure the structural safety by verifying its resistance to dynamic forces.

INTRODUCTION

Currently, more than 2,000 different hydraulic structures are operating in the territory of the Republic of Karakalpakstan. In the reliable and efficient operation of these facilities for large consumers of such sectors of the economy as agriculture, drinking water supply, and fishing, it is important to ensure their uninterrupted operation and safety. Since the structures being operated are located in complex climatic and geological-hydrogeological conditions, constant monitoring of their uninterrupted and accident-free operation is of practical importance [1-7].

The water discharge structure into the Birlik Canal, which is the object of research, was built in 1970 at the Tabankul Hydraulic Unit from monolithic reinforced concrete. The water outlet structure is located to the left of the barrier structure and is designed to have a capacity of 20 m^3/s. The structure has a two-point pipe with a length of 50 m. The dimensions of the holes are 2.5x2.5 m. Two flat sliding gates measuring 2.5x2.5 m with single-helical electrified lifts are installed at the entrance. The connection with the upper and lower befs is made by reverse walls. The lower reach, 50 m long, is reinforced with concrete. The Risberma is 25 m long and is attached to a reinforced concrete lattice with a boulder.

There are no specially installed control and measuring devices at the water discharge structure. The lifting of gates is carried out manually. For more than 50 years of operation, no geodetic measurement work has been carried out to determine the settlement and displacement of structures. Due to the passage of various types of heavy loads and light vehicles weighing over 5 tons through the structure, a process of subsidence of the crest, body, and base of the structure is observed. Particularly intensive subsidence was observed in the lower part of the structure's ridge. There are cracks and breaks in the concrete parts of the structure. The channel bed and sides are eroded, and the front of the structure and the channel bed are covered with silt. Defects and displacements were observed on the fastening plates. The flat gates were subjected to corrosion (Fig. 1). During the movement of heavy and light vehicles in the structure, dynamic forces arose. Dynamic forces led to the formation of cracks in the concrete, vibration of shut-off mechanisms, weakening of fasteners, and especially the loss of structural stability. Therefore, ensuring safety by checking the stability of the structure for dynamic forces is relevant [8].

In all calculations of “structure-base” system loads, ensuring the stability of structures and the strength of the base, stress-strain states are taken into account. With a complex geological structure of the structure's bases, it is recommended to use the finite element method for calculating the uneven settlement of the structure. This method has

been widely used recently and allows for the study of static and dynamic problems of elasticity theory for homogeneous and inhomogeneous bases of various configurations.

a)  b) 

FIGURE 1. Deformations arising in the technical condition of the structure
a) defects in plate fasteners, b) settlement in the lower part of the structure's ridge

MATERIALS AND METHODS

Calculations of the stress-strain state are a necessary element of structures and their subsequent monitoring during operation. Such calculations allow for finding cost-effective and reliable engineering solutions, timely diagnostics, and planning of measures aimed at eliminating negative consequences.

Since the base of the structure is not homogeneous, its physical and mechanical properties are considered as a problem of the modulus of elasticity (Fig. 2).

The different areas of the system's physical and mechanical parameters are indicated by numbers:

(1) for a section of a concrete structure: E=20000 MPa; ρ=2.5 t/m^3; ν=0.3;

(2) for heterogeneous soil: sandy loam - E=17000 MPa; ρ=1.91 t/m^3; ν=0.3; loamy clay - E=16000 MPa; ρ=1.92 t/m^3; ν=0.3; dusty sand - E=18000 MPa; ρ=1.85 t/m^3; ν=0.3.

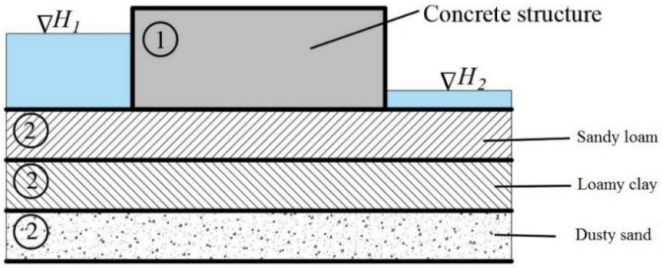

FIGURE 2. Model of the “structure-base” system

In the mathematical formulation of the problem of the dynamic state of a heterogeneous system, the variational principle is used, according to which the sum of the work of all forces (elasticity, inertia, weight, and hydrostatic pressure) during possible displacements is equal to zero [9-11]:

$$\delta A = -\sum_n \left(\int_{V_n} \sigma_{ij} \delta \varepsilon_{ij} dV - \int_{V_n} \rho_n u \delta u dV + \int_{V_n} f_n \delta u dV \right) + \int_S p \delta u dS = 0 \qquad (1)$$

i,j=1,2,3

where u, ε_{ij}, σ_{ij} – respectively the displacement vector, strain and stress tensors; ρ_n – system densities; for the index n, the following values are taken: for the structure n=1, for the base region n=2; f_n – mass (weight) force vector; p – hydrostatic pressure on the surface of the system in contact with water.

When using the finite element method, the system under consideration is divided into finite elements, which in this study are taken as rectangles. Within the element, approximating displacement functions are given. Figure 3 shows the type of rectangular element and approximating functions used, the degree of which is equal to 8 (each node has 2). Here, bi are unknown parameters. These parameters are determined from the permissible nodal displacements of the element as a result of performing the finite element method procedure. The stiffness and mass matrices for a rectangular element are given in the literature using the finite element method [10-14].

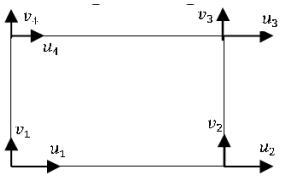

FIGURE 3. Rectangular finite element with approximating displacement functions

$$\begin{aligned} u &= b_1 + b_2 x + b_3 y + b_4 xy \\ v &= b_5 + b_6 x + b_7 y + b_8 xy \end{aligned} \tag{2}$$

To obtain a system of equations solved by the finite-element discretization method, the elements are combined at the nodal points, and their displacements are solutions of the variational equation (1), which realizes the minimum functional of the work [15]. The resulting system of differential equations (excluding dissipation) has the form:

$$[M]\{u\}+\{K\}[u]=\{P(t)\}, \text{ where } \{P(t)\}=[M]\{u_0\} \tag{3}$$

where [K], [M] – rigidity and mass matrices of the entire system, formed from the corresponding matrices of individual elements; $\{u\}$ – required node displacement vector; $\{u_0\}$ – base acceleration.

Equation (3) is solved stepwise using the Newmark method, and based on the displacements of the nodal points obtained during its solution, the displacements within each element are determined, and then the deformations in the elements are determined using the Cauchy equations.

The dynamic effect is shown as a two-part harmonic acceleration of the base, acting along both the horizontal and vertical directions [16,17].

Harmonic acceleration at the lower boundary of the system is used as the input effect.

$$\left.\begin{aligned} u_0 &= A\sin(2\pi\omega t) \\ v_0 &= B\sin(2\pi\omega t) \\ A &= B = 1\text{м}/c^2 \end{aligned}\right\} \tag{4}$$

The indicated amplitude values (A and B) correspond to a 7-point system (0.1 g m/s). According to the spectral method of dynamic calculation of the water release structure for kinematic impact, the dynamic load can be determined by the following formula [17]:

$$S_{ik} = G_k A\, \beta_i \eta_{ik} \tag{5}$$

where G_k – mass corresponding to the k-th node; A – calculated seismicity (0.1 - 7 points, 0.2 - 8 points, 0.4 - 9 points); β_i – dynamicity coefficient (inverse proportional to the period of natural vibrations); η_{ik} – coefficients of natural forms, normalized by the mass obtained when solving the problem for natural values.

Thus, the first step in dynamic calculations is to find the main frequencies and forms of natural vibrations of the studied object, which are included in the formula for the conditional seismic load. The dynamic characteristics of the

system are determined in the absence of dynamic loads. In this case, the finite element method leads to the solution of the dynamic problem about the natural frequencies and forms of oscillations, as well as to the solution of the vector problem corresponding to the natural values (ω) – natural frequencies and $\{u\}$ – natural form:

$$([K] - \omega^2[M])\{u\} = 0 \quad (6)$$

Based on the forms obtained in the process of solving the system representing the displacements of the nodal points (using the approximating functions shown in Fig. 3), the displacements within each element are determined, and then the deformations in the elements are determined using the Cauchy equation, and the stresses are determined based on the obtained deformations [18,19].

RESEARCH RESULTS

In Figure 4, the regions of maximum stress for both forms of natural vibrations are shown in dark color. In both cases, this area in the drawings corresponds to the weakened area (complex-layered soil base), where the greatest stresses arise due to the greatest deformations of the area shown in the main forms. The first two forms of natural oscillations, obtained by the Muller method based on the finite element grid, are given, indicating their corresponding frequencies and periods.

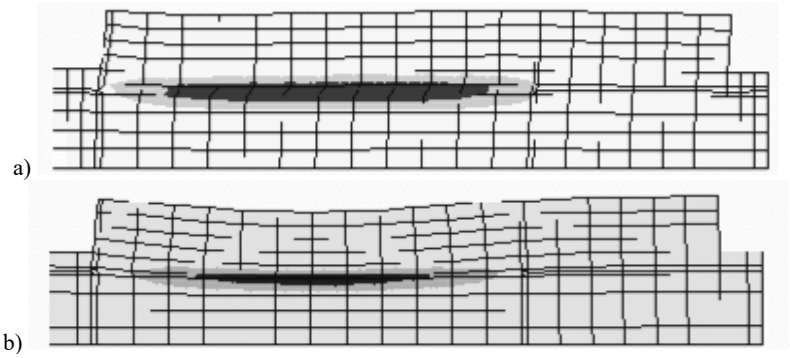

FIGURE 4. Maximum stresses in the system of the first (a) and second (b) forms of natural oscillations based on a deformed finite-element mesh

a) tangential stresses of the first form of oscillation (horizontal displacement). Maximum tangential stresses (0,19 MPa) are in the weakened region. Period T_1=0,061 sec, frequency ω_1=16.4 Hz.

b) vertical stresses of the second form of oscillation. Maximum stresses (0,22 MPa - compression) are in the weakened region. Period T_2=0,048 sec, frequency ω_2=20.4 Hz.

The first form arises as a result of the displacement of the upper boundary of the soil layer relative to the lower boundary, resulting in shear deformation and, accordingly, large tangential stresses, as shown in Figure 4a. The second figure represents the compression of the weakened area under the weight of the upper area and, accordingly, large vertical stresses (Figure 3b). In both cases, the deformation of the lower soil layer is insignificant. Thus, the weakened area is the most deformable part of the system, in which significant tangential and normal stresses are concentrated, which can lead to the destruction of layers located near this area.

Based on the obtained dynamic characteristics, it is possible to predict the state of the structure and the stress-strain state under frequency-kinematic influences.

Consequently, if the influence has a frequency corresponding to the frequency of the system's natural oscillations, then the system transitions to resonant oscillation mode: horizontal, if $p=\omega_1$, or vertical, if $p=\omega_2$.

The displacement of system points under kinematic influence is determined by solving the system of equations (2). In this study, the displacement is determined by the stepwise Newmark method, which is determined based on the decomposition of $u(t_i+\tau)$ into a series according to the degrees of the integration step τ and parameters, which ensures unconditional convergence of the integration process with $\beta \geq 0{,}5$; $\alpha \geq 0{,}25(\beta+0{,}5)^2$ and a zero initial condition [17]:

$$u(t_i+\tau)=u_i+\tau\cdot u_i+\frac{\tau^2}{2}u_i+\alpha\cdot\tau^3u_i;\ u(t_i+\tau)=q_i+\tau\cdot u_i+\beta\tau^2u_i \quad (7)$$

The displacement of points at the edges of the weakened area (A,B) and the lower edges of the structure (C,D) under horizontal influence with the first natural frequency of the system is shown in Figure 5.

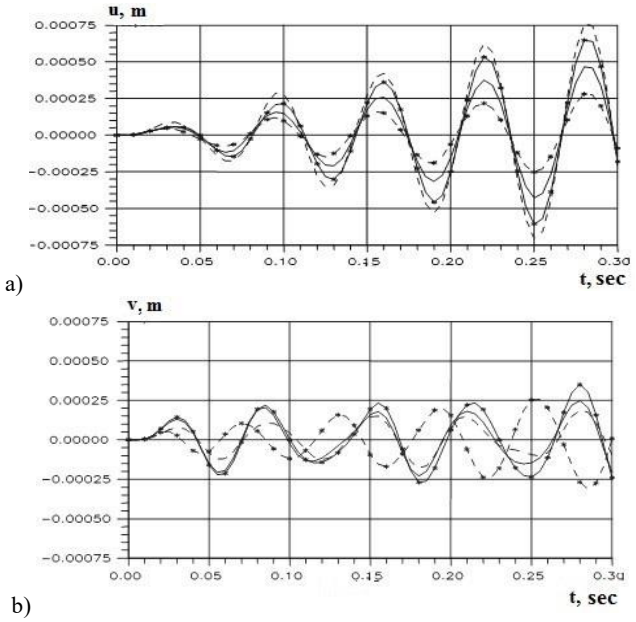

FIGURE 5. Horizontal (a) and vertical (b) displacements of points:
A (————), B (- - - -), C (—x—x—), D (- x - x - x -) under the influence of the fundamental frequency of natural vibrations

Analysis of the obtained results shows that when interacting with the fundamental frequency of natural vibrations, the horizontal displacements occur synchronously, and their amplitude increases linearly (Fig. 5a). The amplitude of vertical oscillations is two times smaller than the amplitude of horizontal oscillations (Fig. 5b), while the oscillations of the lateral faces of the structure become non-synchronous over time (point D (- x - x - x -) and point C (—x—x—)). This is explained by the asymmetrical location of the weakened zone under the structure. The results in the figure were obtained for only four points, excluding damping in the soil: two along the edges of the weakened zone and two to the left and right of the structure's base.

Thus, with an external influence with a frequency corresponding to the first, fundamental, natural frequency of the system under consideration, its motion is described by oscillations whose amplitude in the horizontal direction is twice the amplitude in the vertical direction. In this case, the elastic system mainly transitions to a resonant oscillation mode in the horizontal direction (Fig. 5a). These results can be characterized as test results confirming the reliability of the calculation, i.e., the occurrence of resonance when the frequency of the impact and the natural frequency of the system's oscillations are equal.

CONCLUSIONS

Based on the criteria for transitioning from an elastic state to a plastic state, it has been established that the most dangerous zone is the zone that changes properties, which is the area of weakening, in which the greatest equivalent stress is recorded. This change led to the greatest deformation of the system. With increasing elastic modulus, the equivalent stresses in the weakened area decrease, and in a homogeneous soil, they are evenly distributed throughout the system.

The dynamic state of the system (horizontal and vertical displacements) with different soil properties under two-component influences causing oscillations along the main forms was investigated:

- when the frequency of external influence coincides with the first natural frequency of the structure, resonance with vertical oscillations is observed in the system, caused by the predominance of horizontal oscillations and the proximity of two main frequencies;
- vertical oscillations prevail when the frequency of exposure is equal to the second natural frequency;
- accounting for friction in the ground leads to damped oscillations of the system after the impact is stopped;
- the asymmetrical location of the weakened zone under the structure leads to the rotation of the structure in the vertical plane.

REFERENCES

1. I. E. Makhmudov, A. A. Mirzaev, A. K. Rajabov, S. M. Musaev, B. B. Ulugbekov. Socio-Economic Impact on Water Conservation Implementation in Uzbekistan. E3S Web of Conferences (2023) 449, pp. 1-7. https://doi.org/10.1051/e3sconf/202344906013
2. K. S. Dzhuraev, N. E. Karimova, B. B. Mahmarasulov. Technical and economic efficiency of pumped storage power plants in Uzbekistan. AIP Conference Proceedings 2552, 030015 (2022). pp. 1-7. DOI: 10.1063/5.0112079
3. D. T. Paluanov. A model for ensuring the safety of hydraulic structures based on computer technology. E3S Web of Conferences 474, 02019 (2024) pp. 1-5. https://doi.org/10.1051/e3sconf/202447402019
4. B. O. Kenjaev, D. T. Paluanov, D. A. Mamatkulov, V. V. Romanova. Methods and technologies for ensuring the reliability of excitation of synchronous generators of small hydroelectric power stations in Uzbekistan. E3S Web of Conferences (2020) 216, 01065, pp. 1-3. https://doi.org/10.1051/e3sconf/202021601065
5. E. Kan, M. Mukhammadiev, K. Dzhuraev, A. Abduaziz Uulu. Assessment of economic efficiency of combined power plants based on renewable energies. E3S Web of Conferences 401, 04005 (2023). DOI:10.1051/e3sconf/202340104005
6. E. Kan, M. Mukhammadiev, K. Dzhuraev, A. Abduaziz Uulu, F. Shadibekova. Methodology for determining technical, economic and environmental performance of combined power plants. E3S Web of Conferences 401, 04036 (2023). DOI:10.1051/e3sconf/202340104036
7. M. M. Mukhammadiev, F. J. Nosirov, K. S. Dzhuraev. Prospects for the development of the use of pumped storage power plants in the energy system of the republic of Uzbekistan. Proceedings of International Conference on Applied Innovation in IT (2023). pp.239-245. DOI: 10.25673/101944.
8. D. Paluanov, D. Mamatkulov, S. Gadaev, F. Saidov. Field research to ensure the safety of the earth dam. E3S Web of Conferences 590, 07001 (2024). pp. 1-7. https://doi.org/10.1051/e3sconf/202459007001
9. M. M. Mirsaidov, T. Z. Sultanov. Assessment of the stress-strain state of earth dams, taking into account nonlinear deformation of the material and finite deformations. Engineering and Construction Journal (2014). pp. 73-82. doi: 10.5862/MCE.49.8
10. K. D. Saliyamova, D. F. Rumi. Transformation of the stress-strain base of a structure with uneven soil moisture. Bulletin of BGTU. (2016). pp. 94-99.
11. K. D. Saliyamova, D. F. Rumi. Numerical analysis of the stress-strain state of the "soil structure-foundation" system. Equipment and Technology (2016). pp. 536-545. DOI: 10.17516/1999-494X-2016-9-4-536-545
12. D. Paluanov, B. Kenjaev, D. Mamatkulov, S. Gadaev. Evaluating vibration causes in vertical hydraulic units of hydroelectric power plants during operation. AIP Conf. Proc. 3331, 040082 (2025). pp. 1-6. https://doi.org/10.1063/5.0305998
13. O. Zenkevich. The Method of Finite Elements in Engineering. M. 541 (1975).
14. V. A. Postnov, I. Y. Kharkhurim. The Method of Finite Elements in Calculations of Ship Structures. L. 342 (1974).
15. P. P. Kulmach. Seismic Resistance of Port Hydraulic Structures (Moscow, 1970).
16. Urban planning norms and rules 2.06.11-04. Construction in seismic districts. Hydraulic Structures (Tashkent, 2006).
17. Guide for Determining Loads and Impacts on Hydraulic Structures (Wave, Ice, and Ships). (Leningrad, 1977).
18. D. T. Paluanov. Construction of low-pressure hydraulic structures. IOP Conference Series: Earth and Environmental Science 1076(2022)012080. pp. 1-5. https://doi:10.1088/1755-1315/1076/1/012080
19. M. M. Mukhammadiev, K. S. Dzuraev, A. Abduaziz uulu, H. Murodov. The use of micro hydroelectric power plants with existing hydraulic systems. AIP Conference Proceedings 2552, 050031 (2022). pp. 1-8. DOI: 10.1063/5.0111916